

Journal of Materials Chemistry A

Accepted Manuscript



This is an *Accepted Manuscript*, which has been through the Royal Society of Chemistry peer review process and has been accepted for publication.

Accepted Manuscripts are published online shortly after acceptance, before technical editing, formatting and proof reading. Using this free service, authors can make their results available to the community, in citable form, before we publish the edited article. We will replace this *Accepted Manuscript* with the edited and formatted *Advance Article* as soon as it is available.

You can find more information about *Accepted Manuscripts* in the [Information for Authors](#).

Please note that technical editing may introduce minor changes to the text and/or graphics, which may alter content. The journal's standard [Terms & Conditions](#) and the [Ethical guidelines](#) still apply. In no event shall the Royal Society of Chemistry be held responsible for any errors or omissions in this *Accepted Manuscript* or any consequences arising from the use of any information it contains.

A DFT Study of Pt Layer Deposition on Catalyst supports of Titanium Oxide, Nitride and Carbide

W11S17: Computational Screening of Supported Metal Films

Xin Xia,^{a*}

*a North China Electric Power University,
No.2 Beinong Road, Beijing, China 102206*

Glenn Jones,^b

*b Johnson Matthey Technology Centre, Pretoria
Building 22, CSIR, Meiring Naude Road, Pretoria, 0184, South Africa*

Misbah Sarwar,^c Qian Tang,^c Ian Harkness,^c David Thompsett^c

*c Johnson Matthey Technology Centre,
Blounts Court, Reading, Berkshire, UK RG4 9NH*

ABSTRACT

Due to carbon corrosion under the electrochemical conditions in PEMFCs, alternative ceramic supports to carbon such as TiO₂ have been considered to improve the environmental resistance and catalyst durability. In this work, a series of metal oxides MO₂ (M=Ti, Ir, Ru), doped and reduced TiO₂ surfaces, titanium nitride and carbide ceramic supports have been chosen to study the Pt deposition behavior using density functional theory. The stacking orders and the electronic screening effect of Pt deposition layers on the different geometric structures of the support surfaces are discussed based on a simple periodic slab model. The structural stability and wetting tendency of Pt overlayers have been estimated via energetic descriptors. The interfacial bonding of catalyst-support has been investigated through the electron density analysis for a group of Ti containing substrates. This suggests a reduced Ti charge state as well as a stronger covalent character of the support material facilitates Pt bonding.

1. INTRODUCTION

Proton exchange membrane fuel cells (PEMFC) are one of the most promising technologies that can provide sustainable power resources for vehicles, stationary and portable applications. The electrocatalyst, which is a key component in PEMFCs, exhibits great influence on the cell reliability and durability, it is also responsible for the high cost that prevents large-scale commercialization of this technology^{[1][2]}. The primary reason for the high cost is as a result of the electrocatalyst being comprised of the scarce of platinum group metals (PGM). The catalytic structure is generally composed of a PGM catalyst layer and an electronically conducting support with high surface area, to maximize the catalyst utilization in the electrodes. Current PEMFCs commonly use nanoporous carbon structures as supports for platinum or platinum based alloy catalysts. However, the carbon support suffers from environmental corrosion and enhanced oxidation rates at high potentials over time, which causes a collapse in catalyst layer structure that can lead to performance decay^[3-5]. This drawback of carbon based materials has prompted great efforts^[3] in searching for alternative ceramic supports that can withstand the corrosive environment, as well as improve the metal catalyst dispersion against dissolution and sintering.

Although the support material is not the active phase where the electrochemical reaction occurs, it provides a physical surface for catalyst dispersion, thereby the support structure greatly influences the performance and durability of the catalyst. The support materials also interact with catalytic metals giving geometric influences on the catalyst stacking order and morphology. To summarise, an ideal catalyst support for fuel cell applications requires some specific properties such as: i) high electrochemical stability under fuel cell operating conditions; ii) adequate electronic conductivity; iii) high metal catalyst dispersion: this requires a strong interaction between the support and Pt film, ideally the Pt should wet the support and enhanced catalytic activity.

Various conductive or semi-conductive ceramic compounds have been studied as catalyst support materials or as a secondary support to modify and promote the

primary catalyst support for PEM fuel cells.^{[3][7-23]} Titanium oxide is one of the most extensively studied and interesting candidates due to its tunable porous surface and distribution, high thermal stability, and mechanical strength. Titania exists in different polymorphs, the most common forms are the anatase and rutile crystal. As a photocatalyst, the anatase TiO₂ is reported to be more efficient than rutile structure.^[6] Regarding to the application in fuel cells, several previous experimental studies^[7-11] suggest that using stoichiometric TiO₂ films as support can control the nanostructure of the catalyst and more effectively disperse the Pt atoms on its surface. The thermal stability of the catalysts and electrochemical activity of Pt on TiO₂ were also found to be better when compared to conventional Pt supported on carbon catalysts.^{[9][10]} However, the low electronic conductivity of TiO₂ is an obstacle that hinders its use in the application. The sub-stoichiometric titanium oxides, such as the oxygen reduced TiO_x structures^[12-15] and metal doped (e.g. Nb)^{[16][17]} TiO₂ have attracted great interest due to their improved electron conductivity as well as the potential for enhanced Pt wetting. The carbonization of TiO₂ forms a titanium oxy-carbide compound^[18], which along with the conductive titanium nitride^{[19][20]} and carbide^{[21][22]} are emerging candidates in the research of catalyst support. However, the mechanism of how these materials work as support structures remains unclear.

In this paper, we reported a theoretical analysis of Pt-support interface. Periodic DFT calculations have been carried out in a systematic way to investigate how the support materials affect the catalyst structure and activity. A series of ceramic supports have been chosen for the modelling comparison, including three groups, which are: I) Rutile MO₂, M=Ti, Ir, Ru; II) Modified TiO₂ surfaces or related structures including Nb doped TiO₂, reduced TiO_x and perovskite SrTiO₃; II) Rock salt structure TiX (X=O, N, C). This allows, the electronic effects of the metal cations, anions and the surface modification for Pt interfacial bonding on the substrates to be discussed between and within different support groups. The wetting behaviour of Pt has been studied using an energetic descriptor of the Pt binding energy with respect to different support surfaces. The electronic structures and electron density of the support material and Pt-support interface were analysed to develop further understanding of the interfacial adhesion behaviour of the Pt deposition layer and the support materials.

2. METHODS

All periodic DFT calculations presented in this work have been performed using the non-local GGA-RPBE functional^{[23][24]} as implemented in the CASTEP code^[25]. Ultrasoft pseudopotentials^[26] were used to replace the core electrons from the calculation with a cut-off energy of 350 eV for the plane waves. All the calculated systems are sampled with Monkhorst-pack k-point meshes of actual spacing $\approx 0.04/\text{\AA}$. The bulk structures of support materials were optimized based on the experimental lattice parameters^[27-34]. The surface structures of the support have been studied using a slab model with vacuum space separation of 25 \AA .

For the MO_2 (M=Ti, Ru, Ir) surfaces, a slab consisting of 4 MO_2 trilayers was used as the support surface for Pt deposition, with the bottom two layers fixed to their bulk positions. The top layers of the slabs, together with the Pt adatoms or overlayers, were relaxed until the forces were less than 0.03 eV/ \AA in any Cartesian direction. The total energy calculations are converged to within 10^{-5} eV/Atom. In order to compare different cleavage surface planes, two low index surfaces of (110) and (100) have been considered for the rutile TiO_2 support. Based on the most stable (110) surface of rutile TiO_2 , the oxygen reduced and Nb-doped forms of TiO_2 substrates^[16] have been created as presented in the Supplementary Information (SI) Figure S1. In the cases of TiX structures^[35], the most stable (100) surface has been employed as the support for Pt atoms. A slab model of five layer thickness was used and the top two layers were allowed to relax along with Pt overlayers. In order to investigate the Pt binding to the support surfaces, Pt deposition was modelled by adding Pt on the support atom by atom, rather than layer by layer. This is analogous to the Atomic Layer Deposition (ALD) method by which thin films of Pt are deposited on the support surface. The calculation details of the support surface models are given in the Supplementary Information (SI).

3. DESCRIPTORS OF STRUCTURE STABILITY AND PT WETTING

Two energetic descriptors, Pt layer binding energy and Pt segregation energy are calculated to study the Pt layer and combined Pt/support structure stability. The Pt segregation energy is defined here as the energy change when moving a Pt layer from the support surface (overlayer) to the subsurface (underlayer).

$$E_{seg}[Pt-MX] = E[Pt-MX]^{overlayer} - E[Pt-MX]^{underlayer} \quad (1)$$

The value of E_{seg} indicates the preference of Pt atoms to form a skin layer above the support MX (M= Ti, Ru, Ir; X=O, N, C) surfaces at a low Pt loading. A negative value suggests that Pt tends to segregate to the surface, whereas a positive value implies the platinum has an energetic preference for going subsurface.

With increasing the Pt loading on the support substrate, the tendency of Pt wetting, i.e. whether Pt deposits as a film on the support or detaches from the support surface to form large Pt particles, has been simply assessed by adding Pt overlayers on the support surface. The Pt binding energy, dE_N , is defined as the binding energy increment for adding one Pt layer on the MX supported Pt catalyst surface:

$$dE_N = E[Pt_N-M]^{tot} - E[Pt_{N-1}-MX]^{tot} - n \cdot E[Pt]_{bulk} \quad (2)$$

where N is the number of Pt overlayers ($N = 1, 2, 3 \dots 6$); n is the number of Pt atoms on the support; One Pt monolayer contains different numbers of Pt atoms due to the various geometry of support substrates, e.g. in the cases of $TiO_2(110)$ and (001) support, 1ML Pt contains 3 and 4 Pt atoms, respectively. This number has been converted to Pt mass loading in the latter section. $E[Pt]_{bulk}$ is the cohesive energy of one Pt atom in the Pt bulk (for the most stable fcc structure).

In the electrochemical working environment of the Fuel Cell, the Pt binding energy dE_N is potential dependent. The energetic descriptors we used here can be readily related to the dissolution potential, which is proposed by Greeley *et al.* in their previous work of metal dissolution study.^[36] $\Sigma^N dE_N$ is equal to the grand canonical free energy but for adding a Pt layer instead of a Pt atom. The binding energy dE_N of Pt can be converted to the dissolution potential of Pt and compared with the standard reduction potential of U^0 .^{[36][37]}

$$dE_N = ne (U^* - U^0) \quad (3)$$

where ne is the electrons transferred during the ORR reaction ($n=2$ via a peroxide pathway of dissociation), U^0 is the standard reduction potential of Pt, U^* is the reversible deposition potential of Pt on the support MX. U^0 is about 1.2eV according to the study of dissolution potential for metal deposition.^[37] However, we choose to

calculate the Pt binding energy instead of dissolution potential in our study, since this value can be easily normalized with surface area when comparing different support structures.

4. RESULTS AND DISCUSSIONS

Through the energetic descriptors defined in above, different types of support materials can be compared quantitatively in terms of the segregation and sintering tendency of the Pt catalysts. Herein, various material structures including rutile, anatase, perovskite and rock salt have been modelled as supports for Pt dispersion. To investigate the electronic effect of the support for the interfacial bond formation, we studied a group of Ti containing substrate materials with different anions of X=O, N, C. Both the rutile (R) and anatase (A) structure TiO_2 have been considered. In addition, the Nb doped and oxygen reduced TiO_2 surface structures have been generated based on the model of pure R- TiO_2 (110) surface to study the effect of surface modification.

1. Pt Overlayer Stability

Firstly, the tendency for Pt to segregate has been calculated for the selected oxide and titanium nitride/carbide surfaces. An example of the Pt overlayer and underlayer models on rutile TiO_2 (110) are illustrated in SI-Figure S2. The calculated segregation energies for 1ML Pt coverage are presented with respect to different support structures in **Figure 1**. Such segregation effects can be expected for Pt deposition on the rutile oxide surfaces as well as for Pt on the Ti metal and the metallic TiO and TiN. For the modified rutile surfaces of oxygen reduced TiO_x and Nb doped TiO_2 (110), the subsurface and surface sites are almost equally favourable for Pt atoms (i.e. $E_{\text{seg}} \sim 0$). For the case of A- TiO_2 (001) and perovskite SrTiO_3 (100) surfaces, a Pt underlayer beneath the support surface is slightly more stable, indicated by a positive value of segregation energy. This non-segregation effect is also suggested for Pt on TiC (001). However, the calculated segregation energy shows dependence on the surface coverage of Pt, i.e. a Pt skin can be more favoured when increasing the Pt mass loading on the support substrate. The segregation energy calculated here gives a simple descriptor to compare whether Pt atoms tend to form a skin or locate at the subsurface sites (encapsulation) of support substrates. However, the dynamics of Pt

diffusion are crucial to a real understanding of the Pt segregation behavior on the support surface.

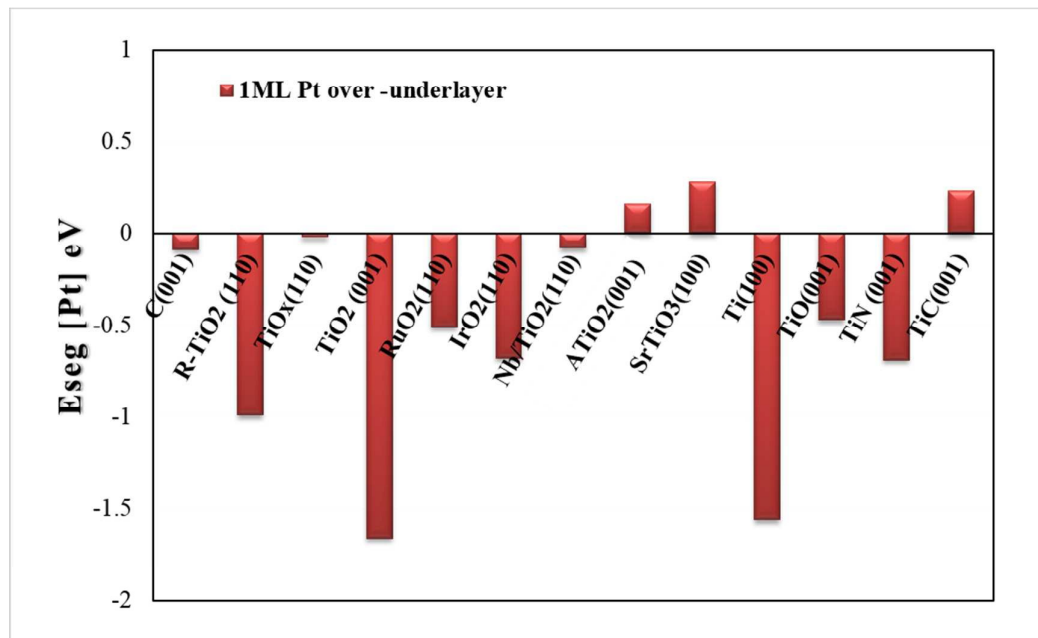


Figure 1. Pt segregation energy for 1ML coverage of Pt on different support materials.

To further study the Pt overlayer stability on the support surface, the tendency of film sintering has been investigated using an energetic term of Pt binding energy increment for adding each Pt layer. The calculation model of Pt wetting is based on the assumption that Pt forms a film structure on the support material during the deposition process. Such a film structure could be energetically stable and will thus wet the support surface. The Pt binding energy increment, dE_N in equation (1), was used here as a descriptor of Pt wetting ability.

This method was first been tested for the study of Pt wetting behaviour on TiO₂ surfaces as given in SI-Figure S5. According to calculations of Pt growth on the TiO₂ surfaces, the addition of the 1st Pt atomic layer on the TiO₂ support requires the highest energy, around 4eV, relative to the cohesive energy of Pt atoms in the fcc bulk structure. The 2nd Pt atom bonds to the first Pt which significantly reduces the energy cost, meaning that the atoms are almost as stable as they would be in the bulk. Small variations of binding energy increment can then be found for Pt in layers less than 4

atomic layers thick. This is considered due to the unsymmetrical structure relaxation of Pt layers. Above 4 layers, the binding energy of Pt converges to its bulk value. The bond formation of the 1st Pt monolayer dominates the deposition process.

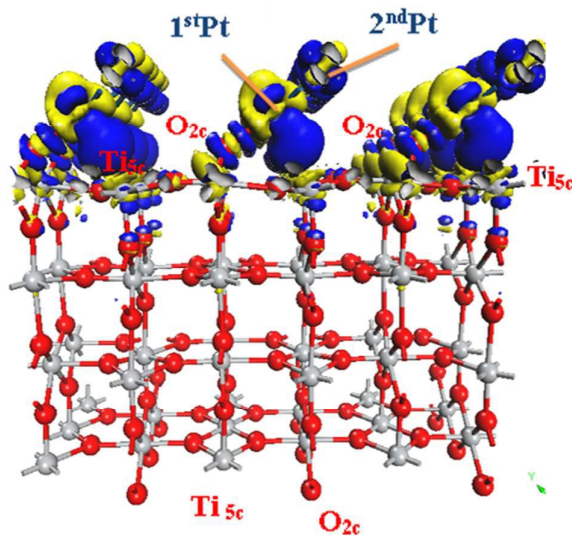


Figure 2 Electron difference analysis of TiO₂ (110) supported Pt overlayer. Two Pt atoms are sited on the TiO₂ (110) surface. Isosurface = $\pm 0.05\text{eV}$ (+blue –yellow)

The geometry and electronic structure of the bond formation of Pt-TiO₂ (110) interface has been further analysed to understand the calculated energies. **Figure 2** shows the electronic density difference of the Pt skin covered TiO₂ (110) and the bare support surface, which indicates the interfacial bond formation to both O and Ti atoms. The preferable Pt adsorption site is on top of 5 fold Ti_{5c} on the surface. Meanwhile, the Pt is slightly negatively charged as presented in **Figure 2**. This calculation results is in accordance with the earlier theoretical literature ^{[38][39]} and experimental studies. ^[40] When adding Pt on TiO₂ (110), the 1st Pt atoms form bonds with both Ti and O ions on the support surface, the 2nd Pt atom tends to form a Pt-Pt bond as in the bulk structure. The high energy cost of the 1st Pt deposition is due to the bond formation of Pt with the bridging sites O_{2c} and Ti_{5c} on the TiO₂ surface.

The electronic influence of the support on Pt layer growth can be further examined by the projected density of states (DOS). An example of how the DOS gradually changes with the Pt layer loadings on TiO₂ (110) is presented in the SI-Figure S6. On the rutile TiO₂ (110), a distorted Pt (211) surface is formed as the Pt layers build up atom by

atom. The DOS of the Pt overlayer converges to a pattern similar to the isolated Pt (211) surface with a slightly shift of the d band centre which is due to the induced lattice strain by the interfacial lattice mismatch. The support material is found to affect the stacking order of Pt overlayers, however, the electronic contribution of the supports only has a minimal effect after 4 overlayers of Pt. This convergence of the Pt overlayer binding energy as well the electronic structures has been observed for all the modelled systems.

We have applied a similar calculation approach to investigate the Pt layer deposition on a range of support candidates. The Pt wetting tendency on each support has been estimated through the calculation of the binding energy increment for Pt overlayers. **Figure 3** plots the binding energy of the N th layer Pt ($N=1, 2, 3\dots$), dE_N as a function of Pt mass loading with the number of Pt atoms converted into Pt mass loading allowing the Pt wetting tendency on different support surfaces to be compared regardless of the surface area. According to **Figure 3**, there is a general trend that can be observed where the binding energy converges to the bulk value of Pt at a thickness of 3-4 deposition layers ($\sim 2 \times 10^{-6}$ g/cm² in Pt mass loading).

In **Figure 3**, $dE_N > 0$ indicates the formation of the isolated bulk phase is more favorable, i.e. sintering of the Pt film may occur. This sintering effect has been predicted for most of the oxide supports, especially rutile MO₂. When altering metal cations (Ti, Ru, Ir) in rutile MO₂ only a small influence on the energetics of Pt wetting were shown. However, since IrO₂ is a metallic oxide whose conduction band is comprised of d electrons from Iridium,^{[41] [42]} the IrO₂ support has shown a dramatically improved conductivity compared to TiO₂ in the same rutile structure. On the reduced oxide R-TiO_x, Nb doped R-TiO₂ and SrTiO₃, which can be viewed as modified TiO₂ surfaces, Pt overlayer stability has been slightly enhanced. The lower value of dE_N suggests a stronger interaction with the support which could promote catalyst dispersion. The TiN and TiC support surfaces require much less energy for Pt layer deposition and growth; therefore, a much better Pt dispersion can be expected for these surfaces. A negative dE_N has been found for TiO support, which suggests Pt will tend to form films and wet the surface of the support. Based on these energetic estimations, the oxidation state of Ti anions at the support surface is considered to

give significant influence on Pt wetting behaviour. To further understand this effect, we analysed the electronic structure of the Ti containing support materials.

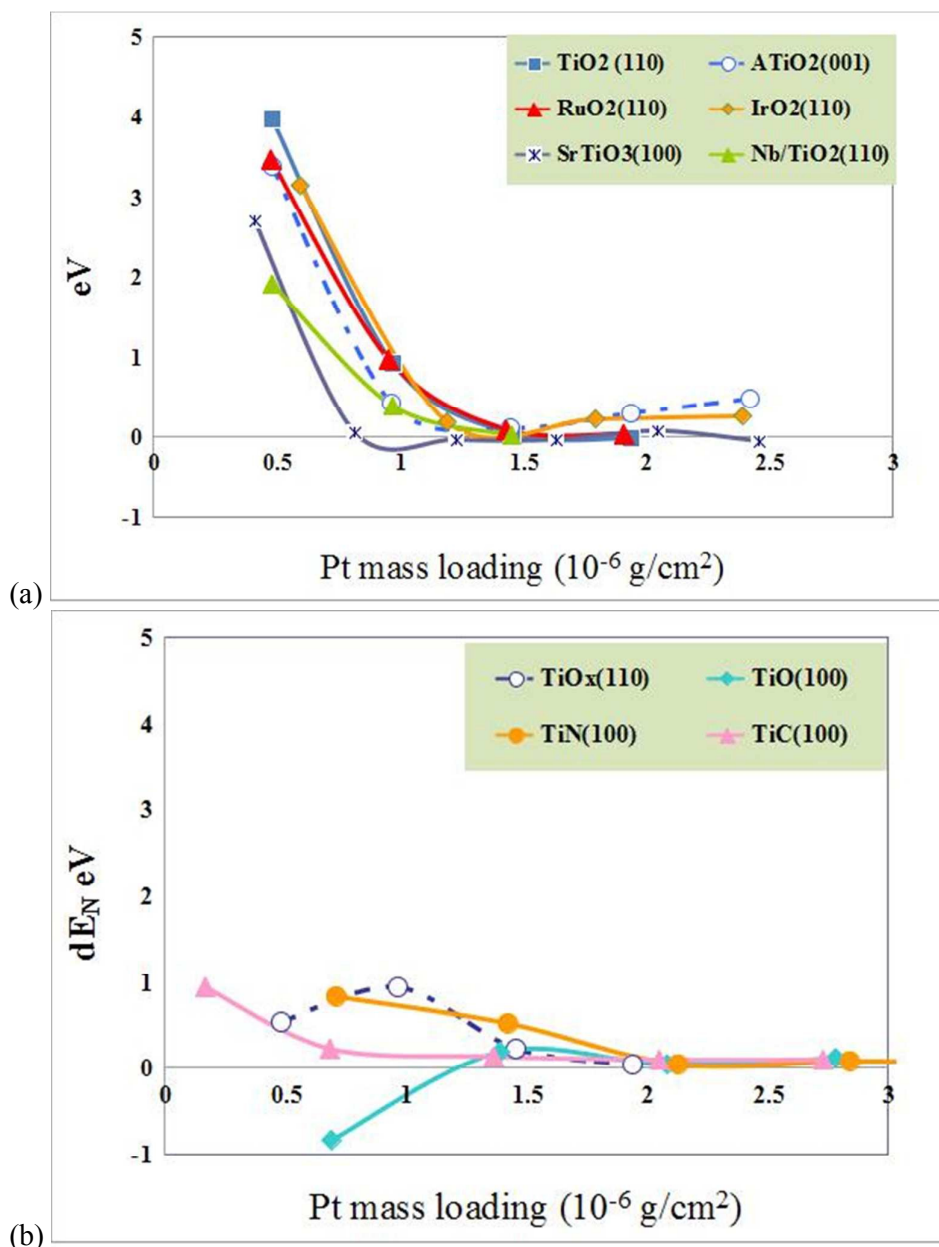


Figure 3 Pt binding energy as a function of Pt film mass loading on (a) MO₂ oxide support surfaces and (b) TiX support surfaces.

II. Electronic study of the interface charge transfer and bonding

The electronic structure has been analysed for a group of Ti-containing supports, which includes the gradually reduced oxidation states of Ti. Since the 1st Pt deposition

layer dominates the interfacial bonding of Pt on the support surface, the electronic structures of the support materials and support covered with 1ML Pt has been investigated to understand the interfacial bond formation and its effect on Pt wetting.

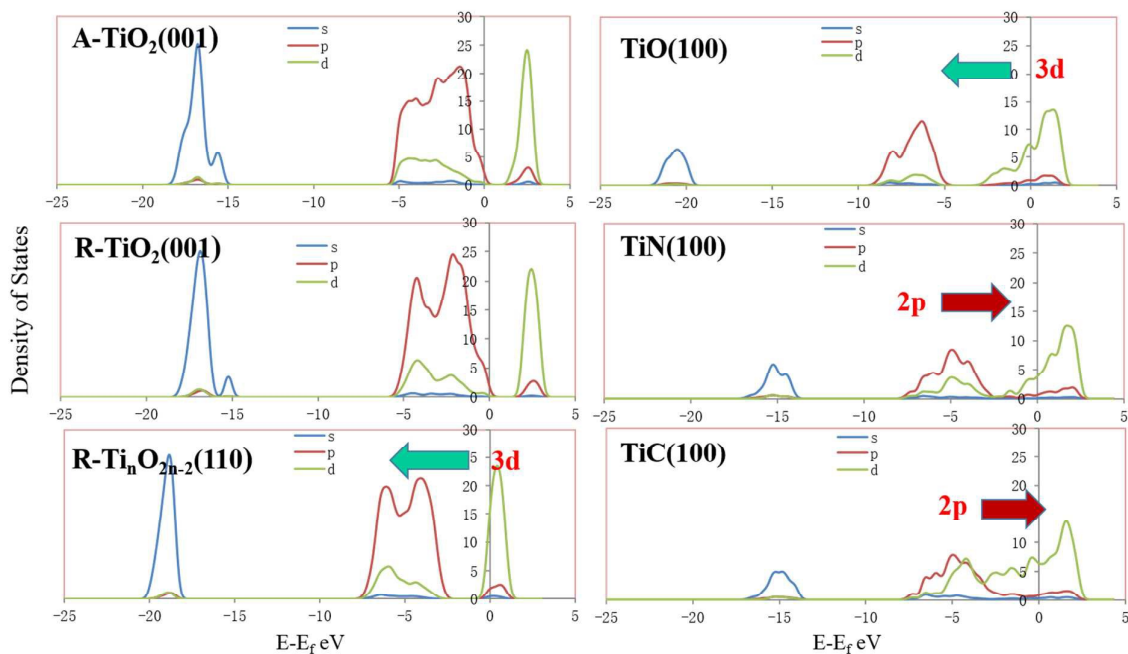


Figure 4. DOS analysis of Ti-containing support surfaces.

Figure 4 compares the DOS diagrams of anatase A-TiO₂(001) and rutile R-TiO₂(110) with two oxygen reduced surfaces, R-Ti_nO_{2n-2}(110) and TiO as well as the rock salt structure TiX (X=O, N, C). The anatase and rutile TiO₂(110) surfaces have a similar DOS, however, the band gap of the calculated rutile surface is slightly smaller, about 0.3eV less than from the anatase. For the oxygen reduced Ti_nO_{2n-2}(110), the energy gap between conduction band (CB) and valence band (VB) has been moved to below the Fermi level. The 3d band of TiO(100) is further delocalized around the Fermi level, which implies an increasing metallic behaviour. The change of electron density distributions in DOS suggests the oxidation state of Ti contributes to the band gap of titanium oxides and might therefore also be expected to influence the bond strength between the supports and Pt. This is particularly evident when one considers the donation or acceptance of electrons from the support by the metallic overlayer. When changing the support anions to those with an increased nuclear charge, the 2p band of TiN and TiC move up towards the Fermi level which results in a much stronger overlapping of C 2p and Ti 3d in TiC.

Based on these Ti containing support models, one Pt atomic layer was built up on the substrate surfaces and relaxed to the most stable configuration. The interfacial charge transfer for different types of Pt-coated support surfaces can be simply compared using the Mulliken charges obtained from DFT calculations (SI-Table S2). The binding effect of Pt on the support surface can be divided into the metal-metal (Pt-Ti) and metal-anion (Pt-X; X=O, N, C) bonds. Since the Mulliken charge is related to the ion electronegativity, the electron transfer calculated in the Mulliken charge can be considered to link with the ionic bonding strength. For Pt supported on the R-TiO₂ (110) substrate, a small fractional charge of 0.06e is transferred from the under-coordinated Ti_{5c} to the adsorbed Pt atom, meanwhile, this Pt atom loses 0.01e to the bridging site oxygen O_{2c}. The interfacial binding effect between the R-TiO₂ (110) substrate and Pt is very weak, and the direction of net charge transfer is from the support to the adsorbed Pt. In the case of Pt deposition on the oxygen reduced R-TiO₂ (110) support, the direction of net charge transfer remains the same, but the amounts of transferred charges are more pronounced, i.e. Pt atom gains 0.40e from Ti and loses 0.21e to surface O. Therefore, a much stronger interfacial bonding between the support and Pt atoms can be expected. The Ti-Pt bond formation was enhanced by reducing the amount of surface oxygen which results in improved wetting behaviour. This effect is further evidenced by the study of Pt deposition on the TiO support, a significant interfacial charge transfer (0.47e from Ti to the adsorbed Pt) indicates Pt wetting occurs more readily. When adding on Pt the non-oxide surfaces of TiN(100), Pt gains electron density from the surface Ti and also attributes a small charge distribution to the neighboring N anion. The direction of charge transfer remains the same as for the oxide support. However, this tendency has been reversed for Pt deposition on the TiC(100) substrate, in which case, Pt obtains 0.16e from the surface C and loses 0.09e to the neighboring site Ti. This noticeable change of charge transfer directions implies different bonding schemes at the Pt-support interfaces, which have been further analyzed by the DOS study.

The electron density distribution of the support surface can significantly affect Pt deposition on it. The DOS of Pt-TiO_n and Pt-TiX (X=O, N, C) are presented in **Figure 5** and **6**, respectively. The DOS of Pt d-band for the three most stable Pt surfaces of (111), (211) and (100) are shown on the left side of the diagram, their d-bands lie between -7 to 1eV with d band centres at around 2 eV. The support DOS

patterns before and after 1 ML Pt deposition are compared by solid and dashed lines in the diagram. When the titanium oxide surface is reduced, the band gap moves down to below the Fermi Level which tends to give a better match with the Pt d-band filling. This results in stronger Pt binding and improved wetting ability on the substrate (sketched in **Figure 5**). Similarly, metal doping on the oxide supports, such as Nb/TiO₂ also moves the d-band down to the Fermi level and enhances Pt wetting. We attribute this to a lower Ti charge state on the support surface which serves to reduce the energy cost for interfacial bonding and benefits Pt wetting.

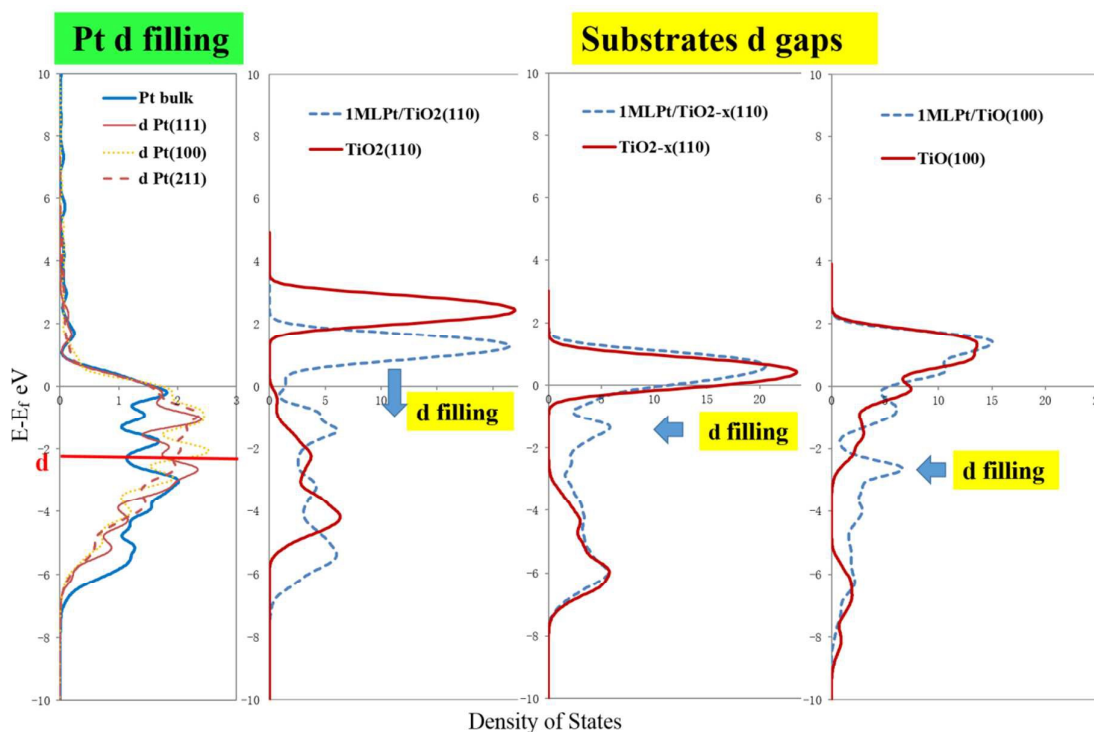


Figure 5. Support d-band filling and TiO_n support d-band gap. The solid (RED) and dashed (BLUE) lines are corresponding to the d band electron density distribution before and after 1ML Pt deposition on the support surfaces, respectively.

In **Figure 6** for the TiX (X=O, N, C) supports, an increasing covalency can be observed moving from oxides to carbides, which is indicated by the stronger overlapping of 2p and 3d orbitals. Due to this delocalization effect, the d-band gap disappears in carbides and Pt binding increases electron density distribution in the range around Fermi Level (as shown in **Figure 6**). Therefore, the bond formation between Pt and the carbide support is manifested by p- and d-orbital overlapping, in contrast with d-band filling in oxides. The change of directions for Mulliken charge

transfer at the Pt and carbide support interface is also a result from the increasing covalency of the carbide support.

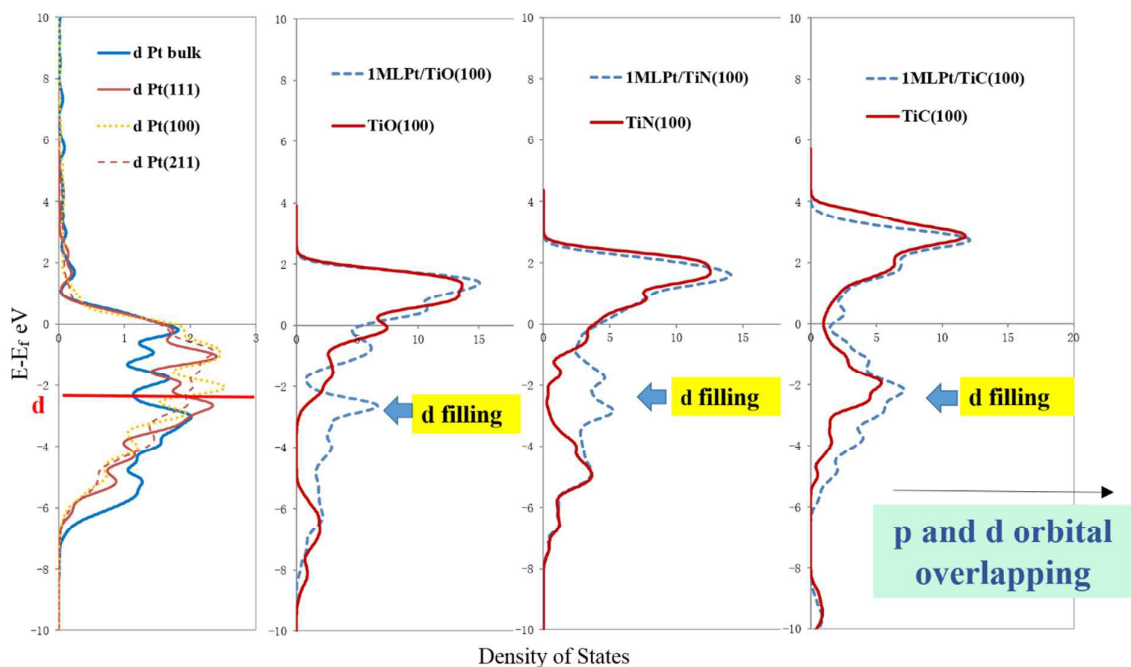


Figure 6. Support d band filling and TiX (X=O, N, C) support d band gap. The solid (RED) and dash (BLUE) lines are corresponding to the d band electron density distribution before and after 1ML Pt deposition on the support surfaces, respectively.

To conclude, a lower oxidation state of Ti in the titanium oxides offers a better match between the Pt d-band centre and support d-band gap and reduces the energy cost of interfacial binding. For nitrides and carbides, stronger covalency delocalizes the support d-band. In which case the interfacial bond formation is more strongly influenced by p and d-orbitals overlapping.

5. SUMMARY AND CONCLUSIONS

The wetting behaviour of Pt on corrosion resistant supports has been studied by DFT. A series of support materials containing titanium oxides with different oxidation states, titanium nitride and carbide structures have been investigated. The energetic descriptors of Pt segregation energy and the binding energy of overlayer growth are used to evaluate the Pt overlayer stability and wetting tendency respectively.

- a) The primary results show that at low Pt loading on the support, a Pt skin is favoured for the rutile oxides. For the modified TiO₂ surfaces, either reduced or metal doped, Pt atoms are less likely to segregate to the support surface. For the titanium nitride and carbide support, the Pt atom has a stronger tendency to go subsurface sites. The Pt film of 4 overlayer thickness has a profound electronic screening effect on the support substrates, which is indicated by the convergences of DOS patterns with Pt overlayer growth. This screening effect is present regardless of support materials.
- b) The Pt wetting behaviour is dominated by the interfacial bond formation of the catalyst-support, arising from the 1st ML of Pt deposition in most cases. By comparing the binding energy of a Pt atom on the support surface to that of a Pt atom in bulk Pt it can be seen that the oxide supports would be expected to be non-wettable due to the high energetic cost of interfacial bond formation. Surface modification such as metal doping or reduction can improve the Pt wetting behaviour.
- c) The analysis of the electronic structure of Ti containing supports suggests the formal +3 oxidation state of Ti gives the d-orbital of the TiO_n support a better match with the d-band filling of the Pt film, by serving to lower the interfacial binding energy. For the covalent compounds of titanium nitride and carbide, the interfacial bond formation is more strongly influenced by p- and d-orbitals overlapping.

ACKNOWLEDGEMENTS

This work was financially supported by Johnson Matthey Technology Centre and Johnson Matthey Fuel Cells. We also acknowledge the North China Electric Power University for the assistance and support.

REFERENCES

- [1] Y. Y. Shao, J. Liu, Y. Wang and Y. Lin, *J. Mater. Chem.*, 19, **2009**, 46.

- [2] H. A. Gasteiger, S. S. Kocha, B. Sompalli and F. T. Wagner, *Appl. Catal. B- Environ.*, 56, **2005**, 9–35.
- [3] E. Antolini, E.R. Gonzalez, *Solid State Ionics* 180, **2009**, 746–763.
- [4] P. Stonehart, *Carbon* 22, **1984**, 423.
- [5] A.M. Couper, D. Pletcher, F.C. Walsh, *Chem. Rev.* 90, **1990**, 837.
- [6] S.Y. Huang, P. Ganesan, S. Park, and B. N. Popov, *J. Am. Chem. Soc.* 131(39), **2009**, 13899.
- [7] T. Luttrell, S. Halpegamage, J. Tao, A. Kramer, E. Sutter and M. Batzill, *Scientific Reports* **2014**, 4, 4043.
- [8] L. Xiong and A. Manthiram, *Electrochim. Acta*, **2004**, 49, 4163.
- [9] H. Q. Song, X. P. Qiu, F. S. Li, W. T. Zhu and L. Q. Chen, *Electrochem. Commun.*, **2007**, 9, 1416.
- [10] J. M. Chen, S. Sarma, C. H. Chen, M. Y. Cheng, S. C. Shih, G. R. Wang, *J. Power Sources*, 159, **2006**, 29.
- [11] S. Kraemer, K. Wikander, G. Lindbergh, A. Lundblad, A. E. C. Palmqvist, *J. Power Sources* 180(1), **2008**, 185.
- [12] J.E. Graves, D. Pletcher, R.L. Clarke, F.C. Walsh, *J. Appl. Electrochem.* 21, **1991**, 848.
- [13] L. He, H.F. Franzen, D.C. Johnson, *J. Appl. Electrochem.* 26, **1996**, 785.
- [14] R.R. Miller-Folk, R.E. Nofle, D. Pletcher, *J. Electroanal. Chem.* 274, **1989**, 257.
- [15] T. Ioroi, Z. Siroma, N. Fujiwara, S. Yamazaki, K. Yasuda, *Electrochem. Comm.* 7, **2005**, 183.
- [16] K. W. Park, K. S. Soel, *Electrochem. Comm.* 9, **2007**, 2256
- [17] J. Arbiol, J. Cerda, G. Dezanneau, A. Cirera, F. Peiró, A. Cornet, and J. R. Morante, *J. Appl. Phys.*, 92, **2002**, 853.
- [18] P. Schmuki et al., *Angew. Chem. Inter. Ed.*, 48, **2009**, 7236.
- [19] B. Avasara, T. Murray, W. Li, P. Haldar, *J. Mater. Chem.* 19, **2009**, 18035.
- [20] B. Avasara, P. Haldar, *Int J. Hydro. Energy*, 36, **2011**, 396574.
- [21] A. Ignaszak, C. Song, W. M. Zhu, J. J. Zhang, A. Bauer, R. Baker, Vladimir Neburchilov, Siyu Ye, S. Campbell, *Electrochimica Acta.* 69, **2012**, 397.
- [22] A. Schlange, A. R. Santos, B. Hasse, B. J.M. Etzold, U. Kunz, T. Turek, *J. Power Sources.* 199, **2012**, 22.
- [23] J. P. Perdew, K. Burke, and M. Ernzerhof, *Phys. Rev. Lett.* 77, **1996**, 3865; 78, **1997**, 1396.
- [24] Y. Zhang and W. Yang, *ibid.* 80, **1998**, 890; J. P. Perdew, K. Burke, and M. Ernzerhof, *ibid.* 80, **1998**, 891.
- [25] S. J. Clark, M. D. Segall, C. J. Pickard, P. J. Hasnip, M. J. Probert, K. Refson, M. C. Payne, "First principles methods using CASTEP", *Zeitschrift fuer Kristallographie* 220(5-6), **2005**, 567-570
- [26] D. Vanderbilt, *Phys. Rev. B*, 41, **1990**, 7892.
- [27] L.F. Mattheiss, *Phys. Rev. B* 13, **1976**, 2433.
- [28] C. Lee, P. Ghosez, X. Gonze, *Phys. Rev. B* 50, **1994**, 13379–13387.
- [29] K. M. Glassford, J. R. Chelikowsky, *Phys. Rev. B*, 46, **1992**, 1284–1298.
- [30] S. C. Abrahams, J. L. Bernstein, *J. Chem. Phys.* 55, **1971**, 3206–3211.
- [31] J. K. Burdett, T. Hughbanks, G. J. Miller, J. W. Richardson, J. V. Smith, *J. Am. Chem. Soc.* 109, **1987**, 3639–3646.

- [32] V. Jeanne-Rose, B. Poumellec, *J. Phys.: Condens. Matter* **11**, **1999**, 1123; Villars, P., Calvert, L. D., Eds. *Person's Handbook of Crystallographic Data for Intermetallic Phases*, 2nd ed.; ASM International: Materials Park, OH, 1991.
- [33] B. A. Hamad, *Eur. Phys. J. B.* **70**, **2009**, 163-169
- [34] V. A. Gubanov, A. L. Ivanovsky, and V. P. Zhukov, *Electronic Structure of Refractory Carbides and Nitrides* ~Cambridge University Press, Cambridge, **1994**.
- [35] M. Marlo, V. Milman, *Phys. Rev. B*, **62**, 2000, 2899.
- [36] J. Greeley, J. K. Nørskov, *Electrochim. Acta* **52**, **2007**, 5829; Jeffrey Greeley, *Electrochimica Acta* **55**, **2010**, 5545.
- [37] Tripkovic, F. Abild-Pedersen, F. Studt, I. Ceri. T. Nagami, T. Bligaard, and J. Rossmeisl, *Chem. Cat. Chem.* **4**, **2012**, 228.
- [38] J. A. Horsley, *J. Am. Chem. Soc.* **101**, **1979**, 2870.
- [39] W.X. Xu, K.D. Schierbaum, W. Goepel, *J. Solid State Chem.* **119**, **1995**, 237.
- [40] S. Takakusagi, K. Fukui, R. Tero, F. Nariyuki, Y. Iwasawa, *Phys. Rev. Lett.* **91**, **2003**, 066102.
- [41] A.K. Goel, G. Skorinko, F.H. Pollak, *Phys. Rev. B* **24**, **1981**, 7342.
- [42] G. K. Wertheim, H. J. Guggenheim, *Phys. Rev. B* **22**(10), **1980**, 4680.
- [43] B. Hammer, L. B. Hansen and J. K. Nørskov, *Phys. Rev. B* **59**, **1999**, 7413.
- [44] L. A. Harris and A. A. Quong, *Phys. Rev. Lett.* **93**, **2004**, 086105
- [45] A. Kiejna, T. Pabisiak and S. W. Gao, *J. Phys.: Condens. Matter* **18**, **2006**, 4207
- [46] S.W. Liu, J.G.Y and M. Jaroniec, *Chem. Mater.* **23**, **2011**, 4085.